

AN ENGINEERING MODEL FOR THE DESIGN OF CUT-BACKS IN RIBBED PANELS

Medhanye Biedebrhan Tekleab¹, Manfred Augustin², Gerhard Schickhofer³

ABSTRACT: This paper deals with the modelling and analysis of ribbed panels with ‘cut-back’ ribs. A critical point in the design of these members is on the determination of the occurring forces and stresses - in particular in tension perpendicular to grain - at the end of the ribs, potentially inducing a splitting failure. Thus, ribbed panels with cut-back ribs in practice always have to be reinforced by appropriate methods (e. g. self-tapping screws or glued-in rods). The open question for the designer is on the determination and the intensity of the design force for the reinforcement.

In this contribution a pure analytical solution procedure based on a simple engineering model has been used. A detailed discussion on modes of load resistance and corresponding deformations has been made, taking into account effects of geometrical & mechanical properties of the components, cut-back length, component-interface properties and load intensity. As a result, simple expressions for the prediction of forces in the reinforcement under transverse loading situations were obtained. All results and discussions may also be applied to systems of beam-beam as well as plate-plate composites with cut-backs and notches of the lower component respectively.

KEYWORDS: CLT, GLT, Stiffening, ribbed-panels, cut-back ribs, shear connection, relative slip, splitting, linear elastic analysis, reinforcement, stresses perpendicular to grain

1 INTRODUCTION

With the increased demand and use of CLT and LVL plates as slabs in structural timber systems, panels with longer spans are desired. One possibility to fulfil the requirements regarding strength, serviceability and economical aspects of long span plates is through the application of wooden ribbed panels. Such structural components consist usually of equally spaced ribs (e.g. glulam) and a plate (e.g. CLT or LVL). These ribs are in general eccentrically glued to the plate along their upper edge (interface line or contact surface).

Ribbed panels/plates with ribs having depths commonly used in practice are regarded as stiffened panels/plates. With relatively deeper ribs, the case of ‘folded plates/structures’, consisting of a system of rectangular cover plate and a sequence of parallel equidistant ribs may come into picture.

2 LOAD-CARRYING BEHAVIOUR

Ribs oriented in the longitudinal direction to increase the flexural stiffness of the plates are due to constructional and economical reasons shorter in length than the longitudinal dimension of the cover plate, i.e. there is a ‘cut-back’ at the end of the ribs. Such ribs are not

supported at the transverse edges of the structural system. The ribs therefore are taking part in the load-carrying process of the complete structural system via distributed ‘interaction’ forces along the interface lines, i.e. interaction shear forces parallel to the interface line & interaction transverse normal forces in the direction orthogonal to the mid-plane of the ribbed panel.

Apart from the usual design of ribbed panels in ULS and SLS this detail requires a special consideration. To get an overview about the phenomenon as well as to calibrate the developed model tests were driven. In Figure 1 the used test configuration is shown, while in Figure 2 the potential failure mode is depicted.

¹ Medhanye Biedebrhan Tekleab,

holz.bau forschungs GmbH, Graz, Austria, medhanye.tekleab@tugraz.at

² Manfred Augustin,

holz.bau forschungs GmbH, Graz, Austria, manfred.augustin@tugraz.at

³ Gerhard Schickhofer,

holz.bau forschungs GmbH, Graz, Austria, and Institute of Timber Engineering and Wood Technology, Graz University of Technology, Austria, gerhard.schickhofer@tugraz.at

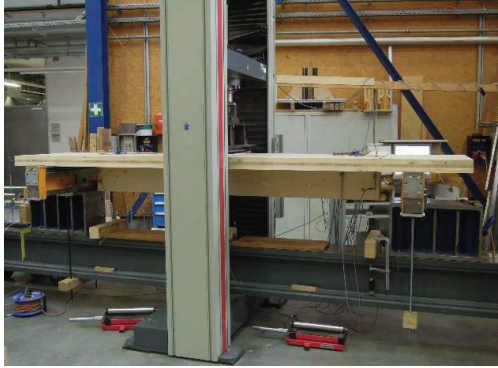


Figure 1: Test configuration



Figure 2: Potential failure mode: 'splitting at the cut-back of the rib'

3 PRACTICAL CONSIDERATIONS

When designing ribbed panels, the usual loadings have to be taken into consideration. In addition, effects from changing moisture contents may occur but are usually neglected in the verification as well as in this paper. While shear forces at the interface are covered (up to a certain limit) by the glue-line, the tension stresses perpendicular tend to induce a splitting-failure at the end of the cut-back. In practise, the resulting tension force has to be taken by appropriate reinforcements (e. g. self-tapping screws or glued-in rods) because of the magnitude and sensitivity of this strength. Currently no specific model for the design of cut-back reinforcements is known.

There have been many studies that directly or indirectly dealt with reinforcements of notches in beam members (see section 5.4) which are to some extent comparable with cut-backs in ribbed panels. Results of such studies have been included in guidelines and standards and are used by practicing engineers. Most studies, if not all, however mix 'transverse tensile stress resultant' as given, for example, in the DIN 1052:1988 [5] formula $F_{t,90} = 1.3 [3(1 - \alpha)^2 - 2(1 - \alpha)^3] V$, which is only valid for unreinforced cases or equivalent, 'force in a given reinforcing screw' referring to any reinforced system irrespective of crack extent or system strength and

'required screwing/reinforcing force' for cases with pre-specified crack extent or intended system strength.

From the viewpoint of practice, one may not definitely speak about avoiding splitting at the end of the cut-back; one may even say cracking at its vicinity is inevitable. Once splitting happens there, the (local) shear resistance will be lost. This effect keeps increasing as crack line grows as a result of load increase.

To cover the requirements in practice, a model for the determination of design forces for the reinforcement of cut-backs in this paper is developed based on a beam model enabling a transparent and understandable design.

4 STRUCTURAL MODELLING

The structural system will be modelled as a plate system with rib stiffeners. The rectangular plate is assumed simply supported along both (parallel) transverse edges and extends to 'infinity' in the other direction (Figure 3).

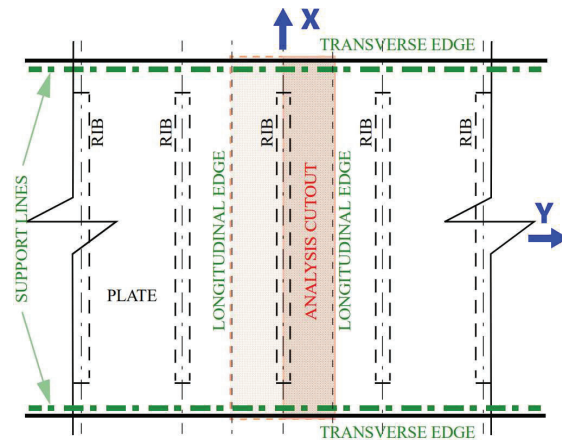


Figure 3: Plan view of the structural system

Due to an assumed independence of the load distribution on the transverse Y-coordinate it becomes possible to reduce the investigation to a suitable analysis 'cut out', applying symmetry conditions along the longitudinal edges of the structural model. The representative analysis 'cut out' will consist of one full rib and a strip of the covering plate composed as T-shaped model (Figure 4). Due to symmetry this model may further be reduced to half of the rib and plate flange. Figure 5 shows sectional views of uncracked and partly cracked interfaces, respectively.

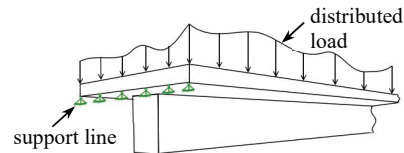


Figure 4: Symmetric T-shaped model

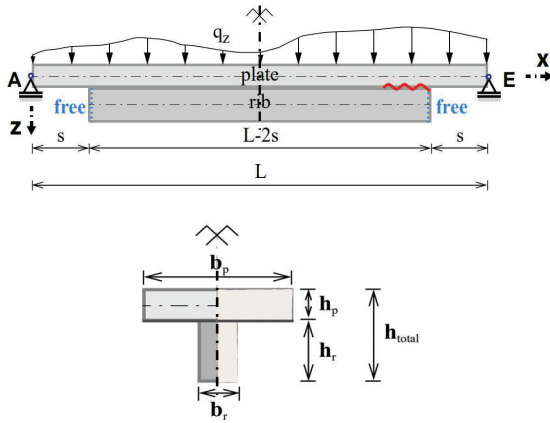


Figure 5: Sectional views: uncracked interface (rib left side) and cracked interface (rib right side) at the cut-back

The first question of interest is how the (linear elastic) structural behavior changes if the support conditions switch from the ‘standard situation’ where ribs are supported alongside the cover plate to the ‘non-standard situation’ where ribs are of the same length as the cover plate but are not supported, i.e. cut-back length $s = 0$. The second question of interest is how this change of behavior will further be affected if the cut-back length ‘ s ’ becomes greater than zero, i.e. $s > 0$ as shown in Figure 10.

5 SOLUTION APPROACH

There will be an interaction of interface shear stress with interface normal stress in resisting applied system loading. For the sake of simplicity, special cases of no relative slip (rigid shear connection) and unrestricted relative slip (without shear connection) have been considered in the current study. Moreover, for simplicity, only bending deformations are considered. Figure 6 shows a substitute system of a general two-element system (cut-back length $s = 0$) that will help to understand the solution approach implemented. In the ‘substitute system’ both elements are first considered supported with a follower step that counterbalances the forces at the free edge of the lower structural element.

In the intermediate step of the ‘substitute system’ where both elements are supported, the load share between the elements depends on their flexural stiffnesses for the case of a system with unrestricted relative slip (without shear connection) as given by Equations (1) and (2).

$$q_{z,1} = \frac{E_1 I_1}{E_1 I_1 + E_2 I_2} q_z \quad (1)$$

$$q_{z,2} = \frac{E_2 I_2}{E_1 I_1 + E_2 I_2} q_z \quad (2)$$

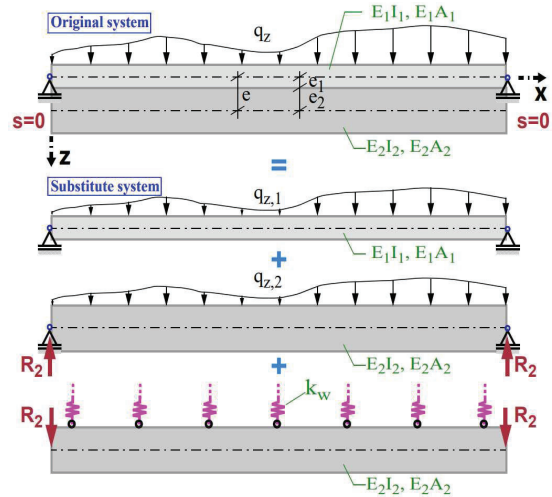


Figure 6: Substitute system and load sharing

For the case of the system with no relative slip (rigid shear connection), the load share between the elements will depend on the axial stiffnesses of the elements in addition to their flexural stiffnesses. The load share in such a case is given by Equations (3) and (4) and the axial force at a section resulting from the stiffness of the interface in shear by Equation (5).

$$q_{z,1} = \frac{E_1 I_1 + \rho e_1 e}{E_1 I_1 + E_2 I_2 + \rho e^2} q_z \quad (3)$$

$$q_{z,2} = \frac{E_2 I_2 + \rho e_2 e}{E_1 I_1 + E_2 I_2 + \rho e^2} q_z \quad (4)$$

$$N_x = -\rho e \frac{\partial^2 w}{\partial x^2} \quad (5)$$

where

$$\rho = \frac{E_1 A_1 \cdot E_2 A_2}{E_1 A_1 + E_2 A_2} \quad (6)$$

It should be noted that for structural components commonly used in practice, the rib contribution towards the system resistance remains almost unaffected when the interface is taken as shear rigid. This is true because the axial stiffness in general has a very small effect when compared with the flexural stiffness.

As far as design of cut-back reinforcement against splitting is concerned, the relative transverse displacement between the plate and rib becomes relevant. For the development of a solution method, a step-by-step procedure based on the superposition of different intermediate steps is proposed.

5.1 ZERO CUT-BACK LENGTH, $s = 0$

As part of the solution, the plate will be analysed and the rib stiffening effects will be introduced as boundary conditions for the plate structure as shown in Figure 7. The basic case where ribs are of the same length as the

cover plate but unsupported (cut-back length $s = 0$) will be considered first.

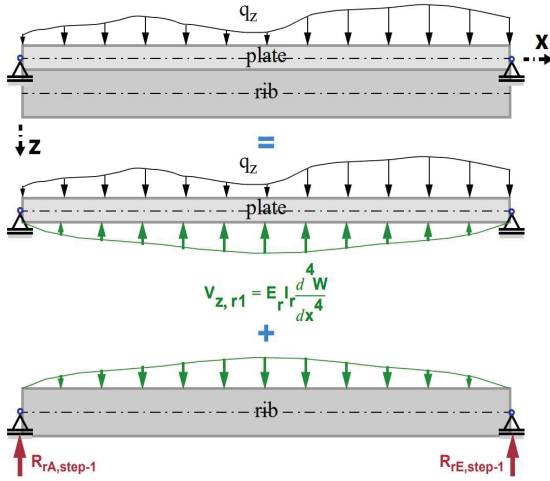


Figure 7: Intermediate structural system: rib-effect as boundary condition

The orthotropic plate differential equation with ‘ w ’ representing the transversal plate bending deformation (downward positive) is given as follows:

$$K_x \frac{\partial^4 w}{\partial x^4} + 2(K_v + 2K_{xy}) \frac{\partial^4 w}{\partial x^2 \partial y^2} + K_y \frac{\partial^4 w}{\partial y^4} = q_z(x, y) \quad (7)$$

where w is the transverse deformation, $q_z(x, y)$ is the transverse distributed loading, K_x and K_y are bending stiffnesses, K_v is coupled bending stiffness, and K_{xy} is torsional stiffness (for CLT, $K_v = 0$ due to cracks & gaps).

5.1.1 First step

As a first step in the solution procedure, Equation (7) can easily be solved taking the following plate boundary conditions into account. In this particular step the ribs, together with the plate, will be considered as simply supported representing a standard simply supported system.

at $x = 0$ and $x = L_r$:

$$w = 0 \quad \partial^2 w / \partial x^2 = 0 \quad (8)$$

at $y = 0$:

$$\frac{\partial w}{\partial y} = 0 \quad V_z = - \left[K_y \frac{\partial^3 w}{\partial y^3} + (K_v + 4K_{xy}) \frac{\partial^3 w}{\partial x^2 \partial y} \right] = \frac{1}{2} E_r I_r \frac{\partial^4 w}{\partial x^4} \quad (9)$$

at $y = b/2$:

$$\frac{\partial w}{\partial y} = 0 \quad V_z = \left[K_y \frac{\partial^3 w}{\partial y^3} + (K_v + 4K_{xy}) \frac{\partial^3 w}{\partial x^2 \partial y} \right] = 0 \quad (10)$$

where V_z = transverse shear force along the edge parallel to X-axis, E_r = rib elastic modulus, I_r = rib moment of inertia and L_r = length of the rib.

In order to fully solve Equation (7), a particular solution w_{part} and a homogeneous solution w_{hom} will be introduced and superposed.

$$w_{p1} = w_{r1} = w_{part} + w_{hom} \quad (11)$$

in which w_{p1} = plate transversal deformation and w_{r1} = rib transversal deformation, both from step-1.

In the following equation, the particular solution w_{part} is shown for a strip acting just like a beam under a constant loading $q_z(x)$ and fulfilling the aforementioned boundary conditions.

$$w_{part} = \frac{q_z}{24 K_x} (x^4 - 2L_r x^3 + L_r^3 x) \quad (12)$$

When Equation (12) is expressed in Fourier series form, it is given by:

$$w_{part} = \frac{4 q_z L_r^4}{\pi^5 K_x} \sum_{1,3,5,\dots}^{\infty} \frac{1}{m^5} \sin \frac{m\pi x}{L_r} \quad (13)$$

and w_{hom} should fulfil the following homogeneous equation:

$$K_x \frac{\partial^4 w}{\partial x^4} + 2(K_v + 2K_{xy}) \frac{\partial^4 w}{\partial x^2 \partial y^2} + K_y \frac{\partial^4 w}{\partial y^4} = 0 \quad (14)$$

For a single span system with hinged end-supports, one can choose a solution for w_{hom} of the type

$$w_{hom} = \sum_{1,3,5,\dots}^{\infty} Y_m \sin \frac{m\pi x}{L_r} \quad (15)$$

where Y_m is a function of y only.

For cases where $(K_v + 2K_{xy})^2 < K_x K_y$, just like in the case of CLT plates, substituting w_{hom} into Equation (14) and solving for Y_m gives:

$$Y_m = \frac{q_z L_r^4}{K_x} (e^{\varphi y} (A_{m1} \cos \psi y + B_{m1} \sin \psi y) + e^{-\varphi y} (C_{m1} \cos \psi y + D_{m1} \sin \psi y)) \quad (16)$$

where

$$\varphi = \frac{m\pi}{L_r} \sqrt{\frac{1}{2} \left(\sqrt{\frac{K_x}{K_y} + \frac{K_v + 2K_{xy}}{K_y}} \right)}, \quad \psi = \frac{m\pi}{L_r} \sqrt{\frac{1}{2} \left(\sqrt{\frac{K_x}{K_y} - \frac{K_v + 2K_{xy}}{K_y}} \right)} \quad (17)$$

The constants A_{m1} , B_{m1} , C_{m1} , and D_{m1} can be found from fulfilling the aforementioned boundary conditions of the plate at $y = 0$ and $y = b/2$. For plates with $K_v = 0$, the expressions for the constants A_{m1} , B_{m1} , C_{m1} , and D_{m1} are given in ANNEX-A.

5.1.2 Second step

The second step will involve balancing/zeroing the end shear of the rib, i.e. re-applying the rib-end reaction forces of the intermediate structural system in the opposite direction. Since this force will result in a fast decaying interface tensile stress (Figure 11) and later be mostly carried by reinforcements very close to the supported edges, it results in very small deformation of the plate. It is thus possible to consider the effects of the tip-loaded rib alone on a beam-on-elastic foundation model.

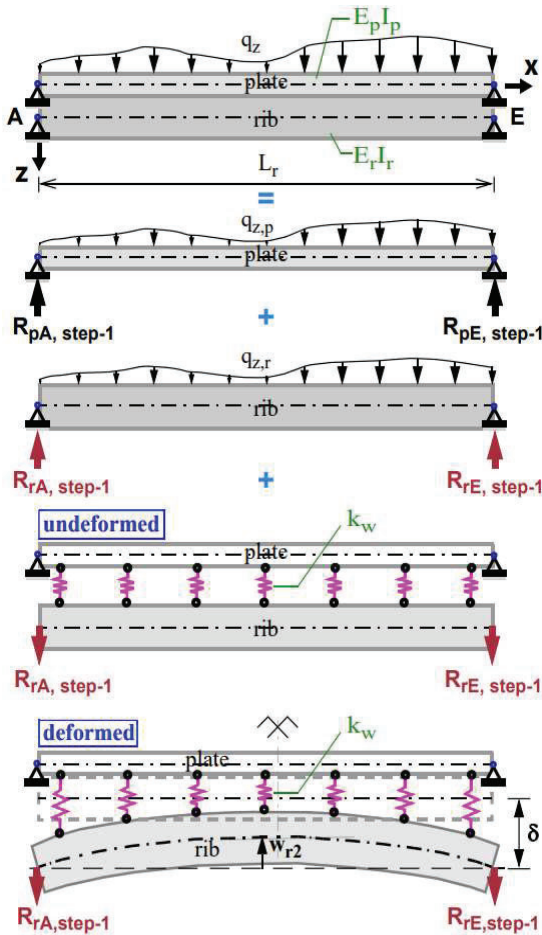


Figure 8: Rib-end shear balancing

The following equation results from equilibrium considerations of the rib:

$$E_r I_r \frac{\partial^4 w_{r2}}{\partial x^4} = k_w (\delta - w_{r2}) \quad (18)$$

where k_w = interface transversal stiffness, δ represents rib-tip transverse deformation of step-2, obtained from force equilibrium equation as given by Equation (19), $R_{r1} = R_{rA, step-1} = R_{rE, step-1}$ is the rib-tip reaction force from step-1 and w_{r2} is rib deformation under rib-tip action R_{r1} (see deformed system, Figure 8).

$$\delta = \frac{1}{L_r} \left(\frac{R_{r1}}{k_w} + \int_0^{L_r/2} w_{r2} dx \right) \quad (19)$$

As part of the second step in the solution procedure, the above differential equation can be solved considering the following rib boundary conditions:
at $x = 0$ and $x = L_r$:

$$\begin{aligned} w_{r2} &= 0 \\ \partial^2 w_{r2} / \partial x^2 &= 0 \end{aligned} \quad (20)$$

The resulting rib transverse deformation will then be given by:

$$w_{r2} = \delta + e^{\lambda x} (C_1 \cos \lambda x + C_2 \sin \lambda x) + e^{-\lambda x} (C_3 \cos \lambda x + C_4 \sin \lambda x) \quad (21)$$

where

$$\begin{aligned} C_1 &= -\frac{1 + e^{\lambda L_r} \cos \lambda L_r}{1 + e^{2\lambda L_r} + 2e^{\lambda L_r} \cos \lambda L_r} \delta, \\ C_2 &= C_4 = -\frac{\sin \lambda L_r}{2(\cos \lambda L_r + \cosh \lambda L_r)} \delta, \\ C_3 &= -\frac{1}{2} \left(1 + \frac{\sin \lambda L_r}{\cos \lambda L_r + \cosh \lambda L_r} \right) \delta, \\ \lambda &= \sqrt[4]{\frac{k_w}{4 E_r I_r}} \end{aligned} \quad (22)$$

The fast-decaying elastic foundation reaction given by $V_{z,r2} = k_w (\delta - w_{r2})$ can also be represented by a Fourier series as follows:

$$V_{z,r2} = \sum_{1,3,5,\dots}^{\infty} E_m \sin \frac{m\pi x}{L_r} \quad (24)$$

where

$$E_m = \frac{32m^3 \pi^3 e^{\lambda L_r} \lambda^4 E_r I_r (\cos \lambda L_r + \cosh \lambda L_r)}{(m^4 \pi^4 + 4\lambda^4 L_r^4) (1 + e^{2\lambda L_r} + 2e^{\lambda L_r} \cos \lambda L_r)} \delta \quad (25)$$

The resultant tensile force of the decaying elastic foundation reaction can then be determined. One is able to compute the total rib boundary effect on the plate and repeat the calculations to determine the plate total deformation.

In the shown form, the mutual deformations of both structural components affect the distribution of forces in the elastic foundation. Since the deformations in the plate at the end of the rib are small, as a simplification, the plate can be assumed rigid. This leads to the structural system of a beam/rib-on-elastic foundation from which the resultant tensile force and the reinforcement force in the region of the cut-back can be determined analytically (Figure 9). The computation of the resultant tensile force of the decaying elastic foundation reaction of such a beam is shown in ANNEX-B.

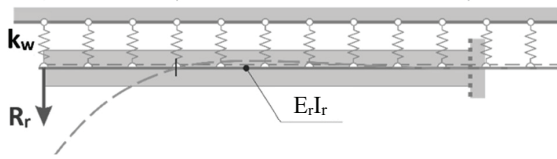


Figure 9: Model for the cut-back based on a beam on an elastic foundation

5.2 NON-ZERO CUT-BACK LENGTH, $s > 0$

The presented structural model can also be used to compute the transverse tensile stress resultants for 'cut-back' lengths larger than zero. Similar to the $s = 0$ case two intermediate steps are involved in the solution procedure.

5.2.1 First step

The first step in the modelling considers a simply supported system (system span length equal to rib span length) with symmetrical end moments obtained by simple mechanics (Figure 10). The rib restraining force/reaction and the corresponding bending contribution of the rib will then be computed.

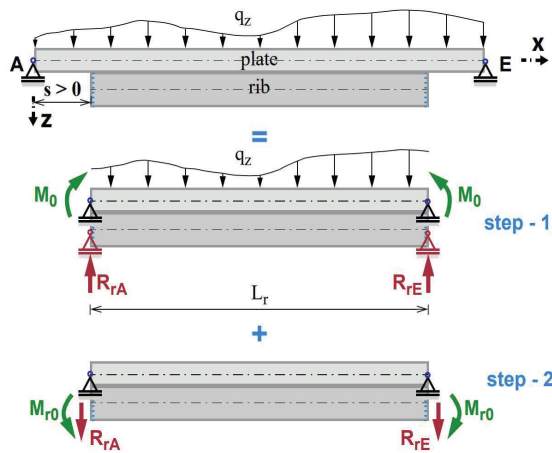


Figure 10: step-by-step solution procedure

5.2.2 Second step

The second step will deal with a rib-tip loaded system that counterbalances the restraining force/reaction and corresponding bending contribution. These are believed to be the main causes for the possible relative displacement between the structural components. It can also be treated as a beam on an elastic foundation.

The resulting interface tensile stress distributions which depend on the interface stiffness against splitting are shown in Figure 11 and Figure 12 for cases with no interface crack and partly cracked, respectively. As can be seen from both figures, the larger the interface tension stiffness is the faster the decay would be. This fact can be related to the need for relatively stiff reinforcement at the cut-back disturbance zone edge.

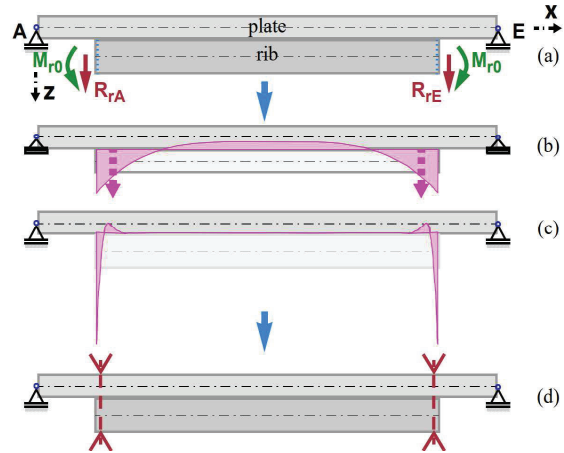


Figure 11: No interface crack: (a) rib-tip actions, (b) transverse stress distribution for smaller interface stiffness, (c) transverse stress distribution for larger interface stiffness and (d) reinforcement

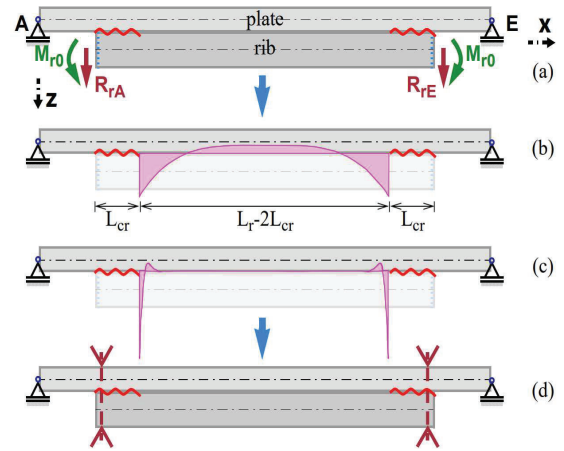


Figure 12: Partly cracked interface (with L_{cr} = crack length): (a) rib-tip actions, (b) transverse stress distribution for smaller interface stiffness, (c) transverse stress distribution for larger interface stiffness and (d) reinforcement

5.3 CALCULATION OF THE FORCE IN THE REINFORCEMENT

The tensile stress resultants (up to the first root) and its distance from the end of the rib can be computed as functions of the applied rib-tip force $R_r = R_{rA} = R_{rE}$ and the moment $M_r = M_{r0} = (E_r I_r / (E_r I_r + E_p I_p)) M_0$ as given by Equations (27) & (28) (see ANNEX-B.1 and ANNEX-B.2). The rib-tip moment M_r is expressed as:

$$M_r = \frac{E_r I_r}{E_r I_r + E_p I_p} \cdot M_0 = \frac{M_0}{1 + \frac{1}{\gamma_r}} \quad (26)$$

It should also be noted that in the following analysis the rib is assumed to be long enough to have enough decay

length for any edge effect, i.e. to avoid effects of one edge on the other.

$$F_{t,90;R_r} = \left(1 + e^{-\frac{\pi}{2}}\right) R_r \approx 1.21 R_r \text{ (for } x_1 = \frac{\pi}{2\lambda}) \quad (27)$$

$$F_{t,90;M_r} = \sqrt{2} e^{-\frac{\pi}{4}} M_r \lambda \approx 0.645 M_r \lambda \text{ (for } x_1 = \frac{\pi}{4\lambda}) \quad (28)$$

In a simultaneous presence of both actions R_r and M_r at the rib-tip, one can compute the combined tensile stress resultant as a rough estimation leading to satisfactory results from the resulting combined stress distribution of the decaying interface tensile stress using Equation (30). In particular this procedure gives results numerically close to the exact solution if the interface stiffness is large. The resultant transverse tensile force for this case is given approximately by Equation (29).

$$\begin{aligned} F_{t,90;R_r+M_r,\text{large } \lambda} &\approx \frac{V}{1 + \frac{1}{\gamma_r}} \left(1 + e^{-\pi/2} + \sqrt{2} e^{-\pi/4} \lambda s\right) \\ &\approx \frac{V}{1 + \frac{1}{\gamma_r}} (1.21 + 0.645 \lambda s) \end{aligned} \quad (29)$$

For general cases, however, the actual transverse tensile stress resultant caused by a simultaneous loading by the rib-tip actions R_r and M_r can be obtained from Equation (30) (see ANNEX-B.3). It represents the tensile stress resultant of the total decaying function up to the first root (zero-point) under the assumption that $M_r \approx R_r \cdot s$.

$$F_{t,90;R_r+M_r} = \frac{V}{1 + \frac{1}{\gamma_r}} (1 + a \cdot e^{-b}) \quad (30)$$

where

$$a = \sqrt{1 + 2 \lambda s (1 + \lambda s)}; \quad b = \tan^{-1} \left(1 + \frac{1}{\lambda s}\right) \dots \text{ [rad]}$$

5.4 COMPARISON WITH KNOWN APPROACHES (VALID FOR BEAMS)

A comparison of results from different approaches (beam theory, DIN 1052-1:1988 [5], Henrici ([6],[7]), draft prEN 1995-1-1:2021 [4]) that dealt with ‘transverse tensile stress resultant’ and the results from the current study have been made. In this context it has to be mentioned, that these studies are valid, from a strict point of view, only for notched beams with rectangular cross-sections, but since no alternatives are known they were used for the comparison.

The expressions used in the following comparison are given by Equations (31) to (35). In the comparison, since no proven methods for the determination of the interface normal stiffness k_w are known yet, the assumption of a constant transverse stress distribution along the rib-depth: $k_w = b_r \cdot E_{90,mean}/h_r$ has been used for the current study.

$$F_{BT} = [3(1 - \alpha)^2 - 2(1 - \alpha)^3] V \quad (31)$$

$$F_{DIN} = 1.3 [3(1 - \alpha)^2 - 2(1 - \alpha)^3] V \quad (32)$$

$$F_{Hen} = \kappa_\beta \kappa_s \kappa_\alpha V \quad (33)$$

$$F_{Tek} = \frac{V}{1 + \frac{1}{\gamma_2}} (1 + a \cdot e^{-b}) \quad (34)$$

$$F_{prEN} = (0.9 + 0.5(2\alpha - 1)^2) \cdot (1 + 2\beta) \cdot (3(1 - \alpha)^2 - 2(1 - \alpha)^3) V \quad (35)$$

where

$$\alpha = h_1/h_{total} \text{ (valid for beams only),}$$

$$\kappa_\beta = 1 + 2\beta,$$

$$\kappa_s = 1 + (s_0 - 1)[1.44(1 - \alpha)(1 - 2\alpha) - 0.1],$$

$$\kappa_\alpha = 1.5(1 - 0.7(1 - \alpha)(3(1 - \alpha)^2 - 2(1 - \alpha)^3)),$$

$$s_0 = \sqrt[4]{E_0/E_{90}} \text{ (in the comparison, } s_0 = 1.81 \text{ is used [6]),}$$

$$\gamma_2 = E_2 I_2 / E_1 I_1,$$

$$\beta = s/h_{total}$$

V ... vertical force

F_{BT} ... force using beam theory

F_{DIN} ... force using DIN 1052-1:1988 [5]

F_{Hen} ... force using Henrici ([6],[7])

F_{Tek} ... force from this study (see Equation (30))

F_{prEN} ... force using prEN 1995-1-1:2021 [4]

Figure 13 shows the comparison for the case of $s/h_{total} = 0.2$ and Figure 14 for the case of $s/h_{total} = 0.4$, where s = cut-back length, h_l = depth of upper element, h_{total} = total depth of the system and V = beam reaction force. For CLT-GLT ribbed panels, the practical range for the h_1/h_{total} -ratio lies between 1/3 and 1/4 [11]. This range is represented by the gray shaded regions in Figure 13 and Figure 14. It can be observed from Figure 13 and Figure 14 that the ‘transverse tensile stress resultant’ decreases with an increase in the h_1/h -ratio, i.e. the stiffening effect from the lower-beam and its contribution to the system strength decreases.

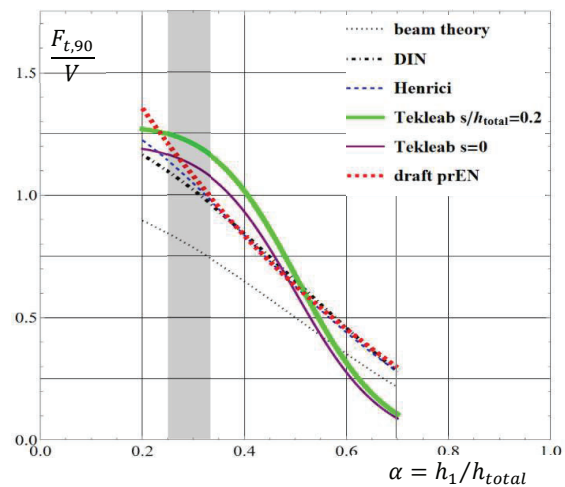


Figure 13: Transverse tensile stress resultants for $s/h_{total} = 0.2$

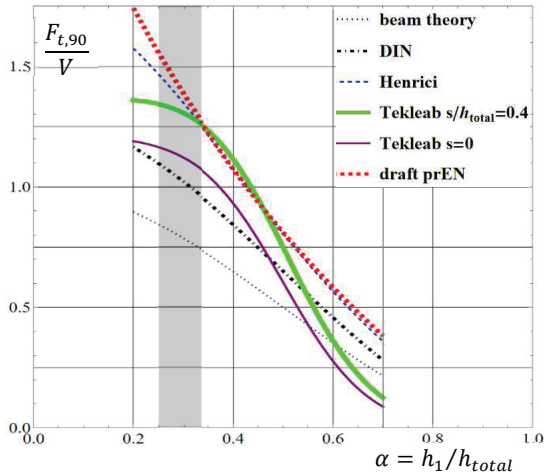


Figure 14: Transverse tensile stress resultants for $s/h_{total} = 0.4$

One can easily recognise from the graphical comparisons that the beam theory and DIN results do not directly include cut-back length effects in addition to the perpendicular to grain stiffness effects.

Figure 15 shows the effect of the cut-back length s on the transverse tensile stress resultant ratio, $F_{t,90}/R_r$, of a system example. It can be seen that with an increasing distance from the supporting line, the transverse stress resultant increases. Due to restrictions of the model this tendency will be valid only for small β -values. Further studies regarding the scope of application are necessary.

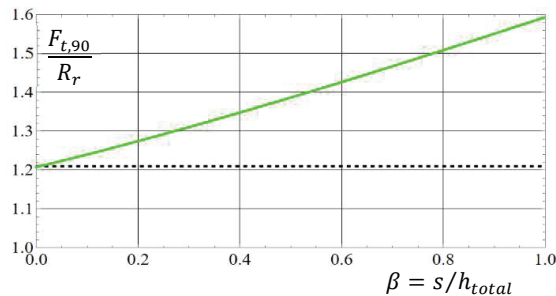


Figure 15: cut-back length effect on tensile stress resultant

The discussions so far dealt with ‘transverse tensile stress resultants’ of unreinforced cases. It is evident that the ‘force in a reinforcement’ is influenced by the tensile load-carrying of the timber and its stiffness as well as the stiffness of the reinforcement. Further efforts on the area will deal with this topic.

6 APPLICATION EXAMPLE

As an example (see Figure 16), a ribbed plate consisting of a glulam rib $b_r/h_r = 160/280$ mm and a 5-layer CLT panel with layer thicknesses of 40-20-20-20-40 mm ($h_p = 140$ mm) and width $b_p = 800$ mm has been considered. The system is a single span simply supported beam with length $L = 10.0$ m and cut-back length $s = 200$ mm. The materials used for the 7-layer combined glulam rib are T21 for the two lower layers & T14 for the upper five

layers and GL24h* for the CLT panel. The system is loaded by its own weight $g_{1,k} = 1.0$ kN/m², a permanent load $g_{2,k} = 2.0$ kN/m² and a live load $q_k = 3.0$ kN/m². It is reinforced with self-tapping screws of $\phi 10/400$ mm at ‘cut-backs’ with an end distance of 50 mm.

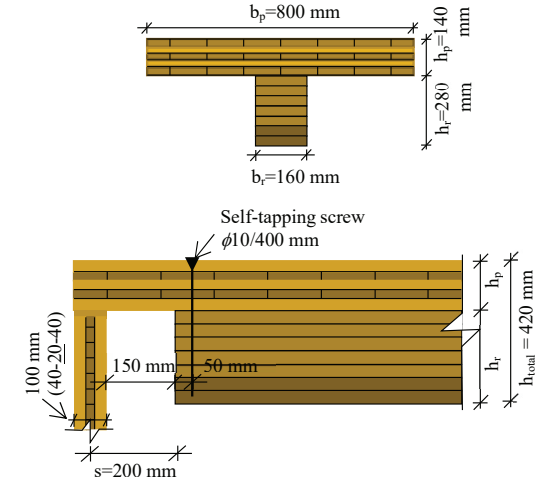


Figure 16: cross-section (upper) and cut-back details (lower)

In order to determine the force in the given screw, one will first obtain the following quantities:

$$q_d = [1.35 \cdot (1.0 + 2.0) + 1.50 \cdot 3.0] \cdot 0.800 = 6.84 \text{ kN/m}$$

$$A_d = \frac{q_d L}{2} = \frac{6.84 \cdot 10.0}{2} = 34.2 \text{ kN}$$

$$V_d = A_d - q_d \cdot s = 34.2 - 6.84 \cdot 0.200 = 32.8 \text{ kN}$$

$$E_p I_p = 1.96 \times 10^{12} \text{ N mm}^2$$

$$E_r I_r = 3.48 \times 10^{12} \text{ N mm}^2$$

$$\rightarrow \gamma_r = \frac{E_r I_r}{E_p I_p} = \frac{3.48 \times 10^{12}}{1.96 \times 10^{12}} = 1.78$$

$$R_{r,d} = \frac{V_d}{1 + \frac{1}{\gamma_r}} = \frac{32.8}{1 + \frac{1}{1.78}} = 21.0 \text{ kN}$$

$$M_{r,d} = R_{r,d} \cdot s = 21.0 \cdot 0.200 = 4.20 \text{ kNm}$$

$$k_w = \frac{b_r \cdot E_{90,mean}}{h_r} = \frac{160 \cdot 300}{280} = 171 \text{ N/mm}^2$$

$$\lambda = \sqrt[4]{\frac{k_w}{4 \cdot E_r I_r}} = \sqrt[4]{\frac{171}{4 \cdot 3.48 \times 10^{12}}} = 0.00187 \text{ [1/mm]}$$

$$- R_{r,d} \text{ and } M_{r,d} \text{ considered solely and added up}$$

$$F_{t,90,d;R_r+M_r,\lambda} \approx 1.21 \cdot 21.0 + 0.645 \cdot 1.87 \cdot 4.20 \approx 30.5 \text{ kN}$$

$$- R_{r,d} \text{ and } M_{r,d} \text{ considered simultaneously}$$

$$a = \sqrt{1 + 2 \cdot 1.87 \cdot 0.2 \cdot (1 + 1.87 \cdot 0.2)} = 1.42$$

$$b = \tan^{-1} \left(1 + \frac{1}{1.87 \cdot 0.2} \right) = 1.31$$

$$F_{t,90,d;R_r+M_r} = 21.0 (1 + 1.42 \cdot e^{-1.31}) = 29.0 \text{ kN}$$

For comparison:

- DIN 1052-1:1988 [5]

$$\alpha = h_{ef}/h_{total} = 140/420 = 1/3$$

$$F_{t,90,d} = 1.3 \cdot V_d \cdot [3(1 - \alpha)^2 - 2(1 - \alpha)^3]$$

$$F_{t,90,d} = 1.3 \cdot 32.8 \cdot \left[3 \left(1 - \frac{1}{3} \right)^2 - 2 \left(1 - \frac{1}{3} \right)^3 \right] = 31.6 \text{ kN}$$

- with DIN 1052 adapted for ribbed panels:

for the composite cross-section: $e_{z,s} = 273$ mm (from the lower edge), $(EI)_{ef} = 2.08 \cdot 10^{13} \text{ Nmm}^2$,

$$F_{t,90,d} = 1.3 \cdot V_d \cdot \frac{b_r}{6} \cdot \frac{E_r}{(EI)_{ef}} \cdot (3 \cdot z_s \cdot h_r^2 - h_r^3)$$

$$F_{t,90,d} = 1.3 \cdot 32.8 \cdot \frac{160}{6} \cdot \frac{12500}{2.08 \cdot 10^{13}} \cdot (3 \cdot 273 \cdot 280^2 - 280^3) = 28.9 \text{ kN}$$

Verification of the reinforcement:

The design resistance per screw is computed applying the following values (screw data from an approval):

- for the verification of the withdrawal resistance: with the withdrawal strength $f_{ax,90,k} = 10.0 \text{ N/mm}^2$, the modification factor $k_{mod} = 0.80$ and the partial safety factor $\gamma_M = 1.30$ for the reinforcement (joint); since the smaller penetration depth is in the CLT plate it becomes crucial for the design.

$$F_{ax,Rd} = k_{mod} \cdot \frac{f_{ax,90,k} \cdot d \cdot l}{\gamma_M} = 0.80 \cdot \frac{10.0 \cdot 10.0 \cdot 140}{1.30} = 8,615 \text{ N} = 8.62 \text{ kN}$$

- for the verification of the screw tensile strength: tensile strength of the screw $F_{tens,k} = 32.0 \text{ kN}$ and the related partial safety factor $\gamma_{M2} = 1.25$.

$$F_{tens,d} = \frac{F_{tens,k}}{\gamma_{M2}} = \frac{32,000}{1.25} = 25,600 \text{ N} = 25.6 \text{ kN}$$

- design resistance per screw:

$$R_{ax,d} = \min\{F_{ax,Rd}; F_{tens,d}\} = \min\{8.62 \text{ kN}; 25.6 \text{ kN}\} = 8.62 \text{ kN}$$

with $n_{ef} = n$, the required screws to cover the force:

$$n_{req} = \frac{F_{t,90,d;R_r+M_r}}{R_{ax,d}} = \frac{29.0}{8.62} = 3.36$$

Applied at each cut-back: $4 \times \text{Ø } 10/400$ mm screws.

The rules regarding spacings and end distances etc. have to be met. Special conditions for the detailing of the reinforcement at the 'cut-back' can be found in ([1], [2]).

7 CONCLUSIONS AND OUTLOOK

Ribbed timber panels are interesting possibility to expand the range of application in timber engineering due to the possibility of realizing floors with larger spans. Because of technical and economic reasons, the ribs of such floor systems are often 'cut-back', i. e. end at a distance from the supports.

The ends of ribs in this case have to be reinforced by appropriate methods (e. g. self-tapping screws). As known to the authors no explicit rules for this mentioned design situation are known or given in relevant standards. Since no alternatives are given, one may use the equations given in the National Annexes to EN 1995-1-1 in Germany and Austria, mentioned for the first time in DIN 1052:1988 [5] for reinforced notches of rectangular cross-sections. It is, however, evident that this approach doesn't cover the given situation of ribbed panels with 'cut-backs' and is thus not valid for this case.

In the current study, simplified expressions for the 'transverse tensile stress resultants' (of unreinforced cases) based on a simple engineering approach applying a beam on elastic foundation were derived. With the developed equations one can easily calculate the force to

be covered by the reinforcement. Since a general approach was used, the presented modelling, analysis and results can also be applied to plate-plate and beam-beam composites. The usual verifications like verifications of bending and shear stresses in ULS as well as deflection and vibration in SLS have to be done. This is important because due to the limited load-carrying capacity of the CLT, too high β -values will not be possible.

In addition to the presented results the interface tensile stiffness, the consideration of shear-deformation effects, interaction of interface shear stress with interface normal stress, non-linear interface behaviour, crack length etc. will be part of the ongoing analysis and experimental research. Moreover, the range of application (regarding α - and β -values) is under investigation. In particular, tests with different lay-ups (γ_r -values and h_p/h_{total} -values) and different β -values are in preparation.

ACKNOWLEDGEMENT

This research work was financed by the Austrian Research Promotion Agency (FFG) and is part of an ongoing study and experimental research on ribbed timber panels being carried out at the competence centre holz.bau forschungs gmbh, Graz, Austria.

REFERENCES

- [1] Augustin, M., et al.: A contribution to the design of ribbed plates, World Conference on Timber Engineering, Vienna, Austria, 2016.
- [2] Augustin, M.: Recommendations regarding the design of CLT ribbed panels. *Research report*, holz.bau forschungs gmbh, Graz, Austria, 2020.
- [3] Bogensperger, T., & Silly, G.: *Zweiachsige Lastabtragung von Brettsperrholzplatten*. Bautechnik, 91(10), 742-752, 2014.
- [4] CEN/TC 250/SC 5 "Eurocode 5: Design of timber structures" consolidated draft prEN 1995-1-1, 2021.
- [5] DIN 1052-1:1988: *Holzbauwerke; Berechnung und Ausführung*. DIN Deutsches Institut für Normung e.V., Berlin, Germany, 1988.
- [6] Henrici, D.: *Beitrag zur Bemessung ausgeklinkter Brettschichtholzträger ein Vergleich mit der DIN 1052*. Bauen mit Holz 11/90, München, Germany, 1990.
- [7] Henrici, D.: *Beitrag zur Spannungsermittlung in ausgeklinkten Biegeträgern aus Holz*. Dissertation, Technische Universität München, München, Germany, 1984.
- [8] Hetenyi, M.: *Beams on elastic foundation, theory with applications in the fields of civil and mechanical engineering*, University of Michigan, 1946.
- [9] Papastavrou, P., et al.: *The design of cross-Laminated timber slabs with cut-back glulam rib downstands – from research to live project*, World Conference on Timber Engineering, 2016.
- [10] Timoshenko S., Woinowsky-Krieger S.: *Theory of plates and shells*. Second edition. McGraw-Hill book company, 1959.
- [11] Wallner-Novak, M., et al.: *Cross-Laminated Timber Structural Design - Volume 2*, proHolz Austria, 2018.

ANNEX-A: Coefficients in Equation (16) for single-span orthotropic plate with constant distributed loading

$$\begin{aligned}
 Am1 &= -\frac{b^5 e^{-\varphi b} \zeta (\varphi^2 + \psi^2) (3\varphi^2 \psi^2 - \psi^4 + e^{\varphi b} (\varphi^2 + \psi^2)^2 + \varphi(\varphi^2 - 3\psi^2)(-\varphi \cos[b \psi] + \psi \sin[b \psi]))}{16L_r^4 \alpha_m^5 (L_r \zeta ((\varphi^2 + \psi^2)^3 - \varphi^2(\varphi^2 - 3\psi^2)(\varphi^2 + \psi^2) \cos[b \psi]) + \psi(4\varphi^2(\varphi^2 - 3\psi^2) \sin[b \psi] - \psi(-3\varphi^2 + \psi^2)(L_r \zeta (\varphi^2 + \psi^2) \cosh[b \varphi] - 4\varphi \sinh[b \varphi]))} \\
 Bm1 &= -\frac{b^5 e^{-\varphi b} \zeta \varphi (\varphi^2 + \psi^2) (-3\varphi^2 \psi + \psi^3 - e^{\varphi b} (\varphi^2 - 3\psi^2)(\psi \cos[b \psi] + \varphi \sin[b \psi]))}{16L_r^4 \alpha_m^5 (L_r \zeta ((\varphi^2 + \psi^2)^3 - \varphi^2(\varphi^2 - 3\psi^2)(\varphi^2 + \psi^2) \cos[b \psi]) + \psi(4\varphi^2(\varphi^2 - 3\psi^2) \sin[b \psi] - \psi(-3\varphi^2 + \psi^2)(L_r \zeta (\varphi^2 + \psi^2) \cosh[b \varphi] - 4\varphi \sinh[b \varphi]))} \\
 Cm1 &= -\frac{b^5 \zeta (\varphi^2 + \psi^2) (e^{\varphi b} \psi^2 (-3\varphi^2 + \psi^2) - (\varphi^2 + \psi^2)^2 + \varphi(\varphi^2 - 3\psi^2)(\varphi \cos[b \psi] + \psi \sin[b \psi]))}{16L_r^4 \alpha_m^5 (L_r \zeta (\varphi^2 + \psi^2) (-\varphi^2 + \psi^2)^2 + \varphi^2(\varphi^2 - 3\psi^2) \cos[b \psi]) + \psi(-4\varphi^2(\varphi^2 - 3\psi^2) \sin[b \psi] + \psi(-3\varphi^2 + \psi^2)(L_r \zeta (\varphi^2 + \psi^2) \cosh[b \varphi] - 4\varphi \sinh[b \varphi]))} \\
 Dm1 &= -\frac{b^5 \zeta \varphi (\varphi^2 + \psi^2) (-e^{\varphi b} \psi (-3\varphi^2 + \psi^2) - (\varphi^2 - 3\psi^2)(-\psi \cos[b \psi] + \varphi \sin[b \psi]))}{16L_r^4 \alpha_m^5 (L_r \zeta (\varphi^2 + \psi^2) (-\varphi^2 + \psi^2)^2 + \varphi^2(\varphi^2 - 3\psi^2) \cos[b \psi]) + \psi(-4\varphi^2(\varphi^2 - 3\psi^2) \sin[b \psi] + \psi(-3\varphi^2 + \psi^2)(L_r \zeta (\varphi^2 + \psi^2) \cosh[b \varphi] - 4\varphi \sinh[b \varphi]))}
 \end{aligned}$$

where $\alpha_m = \frac{b m \pi}{2 L_r}$ and $\zeta = \frac{E_r I_r}{K_x L_r}$

ANNEX-B:

B.1: Semi-infinite Euler-Bernoulli beam with beam-end concentrated force

Deflection: $w(x) = \frac{2 \cdot \lambda \cdot R_r}{k_w} \cdot e^{-\lambda \cdot x} \cdot \cos(\lambda \cdot x)$ with $\lambda = \sqrt[4]{\frac{k_w}{4 \cdot E_r I_r}}$

Position of the first root (zero-point):

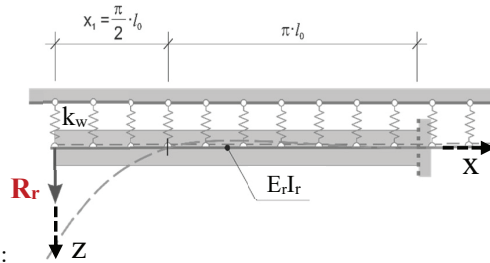
$$w(x) = \frac{2 \cdot \lambda \cdot R_r}{k_w} \cdot e^{-\lambda \cdot x} \cdot \cos(\lambda \cdot x) = 0 \Rightarrow e^{-\lambda \cdot x} \cdot \cos(\lambda \cdot x) = 0 \Rightarrow \cos(\lambda \cdot x) = 0$$

$$\Rightarrow x_1 = \frac{\pi}{2 \cdot \lambda} = \frac{\pi}{2} \cdot \sqrt[4]{\frac{4 \cdot E_r I_r}{k_w}}$$

Integral up to the distance of the first root (= tensile stress resultant):

$$\begin{aligned}
 F_{t,90} &= \int_0^{x_1} \bar{p}(x) dx = 2 \cdot \lambda \cdot R_r \cdot \int_0^{x_1} e^{-\lambda \cdot x} \cdot \cos(\lambda \cdot x) dx = 2 \cdot \lambda \cdot R_r \cdot \left[\frac{e^{-\lambda \cdot x}}{2 \cdot \lambda} \cdot (\sin(\lambda \cdot x) - \cos(\lambda \cdot x)) \right]_0^{x_1} = \\
 &= R_r \cdot \left[\left(e^{-\lambda \cdot x_1} \cdot \left(\frac{\sin(\lambda \cdot x_1)}{1} - \frac{\cos(\lambda \cdot x_1)}{0} \right) - e^{-\lambda \cdot 0} \cdot \left(\frac{\sin(\lambda \cdot 0)}{0} - \frac{\cos(\lambda \cdot 0)}{1} \right) \right) \right] = R_r \cdot [1 + e^{-\lambda \cdot \frac{\pi}{2 \cdot \lambda}}] = 1.21 R_r
 \end{aligned}$$

where $R_r = q_z \cdot \frac{b \cdot l}{2} \cdot \frac{1}{1 + \frac{1}{\gamma_r}}$ and $F_{t,90} = 1.21 \cdot q_z \cdot \frac{b \cdot l}{2} \cdot \frac{1}{1 + \frac{1}{\gamma_r}}$ with $\gamma_r = \frac{E_r I_r}{E_p I_p}$



B.2: Semi-infinite Euler-Bernoulli beam with beam-end concentrated moment

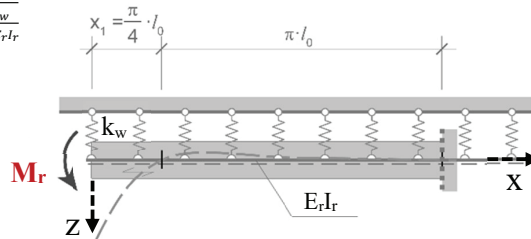
Deflection: $w(x) = \frac{2 \cdot \lambda^2 \cdot M_r}{k_w} \cdot e^{-\lambda \cdot x} \cdot [\cos(\lambda \cdot x) - \sin(\lambda \cdot x)]$ with $\lambda = \sqrt[4]{\frac{k_w}{4 \cdot E_r I_r}}$

Position of the first root (zero-point):

$$w(x) = \frac{2 \cdot \lambda^2 \cdot M_r}{k_w} \cdot e^{-\lambda \cdot x} \cdot [\cos(\lambda \cdot x) - \sin(\lambda \cdot x)] = 0$$

$$\Rightarrow e^{-\lambda \cdot x} \cdot [\cos(\lambda \cdot x) - \sin(\lambda \cdot x)] = 0 \Rightarrow \cos(\lambda \cdot x) - \sin(\lambda \cdot x) = 0$$

$$\Rightarrow x_1 = \frac{\pi}{4 \cdot \lambda} = \frac{\pi}{4} \cdot \sqrt[4]{\frac{4 \cdot E_r I_r}{k_w}}$$



Integral up to the distance of the first root (= tensile stress resultant):

$$\begin{aligned}
 F_{t,90} &= \int_0^{x_1} \bar{p}(x) dx = 2 \cdot \lambda^2 \cdot M_r \cdot \int_0^{x_1} e^{-\lambda x} \cdot [\cos(\lambda \cdot x) - \sin(\lambda \cdot x)] dx = 2 \cdot \lambda^2 \cdot M_r \cdot \left[\frac{e^{-\lambda x}}{\lambda} \cdot \sin(\lambda \cdot x) \right]_0^{x_1} = \\
 &= 2 \cdot \lambda \cdot M_r \cdot \left[\left(e^{-\lambda x_1} \cdot \left(\frac{\sin(\lambda \cdot x_1)}{1/\sqrt{2}} \right) - \frac{e^{-\lambda \cdot 0}}{1} \cdot \left(\frac{\sin(\lambda \cdot 0)}{0} \right) \right) \right] = M_r \cdot \lambda \cdot \left[\sqrt{2} e^{-\lambda \frac{\pi}{4\lambda}} \right] = \mathbf{0.645 M_r \cdot \lambda}
 \end{aligned}$$

B.3: Semi-infinite Euler-Bernoulli beam with beam-end concentrated force and moment

Deflection: $w(x) = \frac{2 \cdot \lambda \cdot R_r}{k_w} \cdot e^{-\lambda x} \cdot \cos(\lambda \cdot x) + \frac{2 \cdot \lambda^2 \cdot M_r}{k_w} \cdot e^{-\lambda x} \cdot [\cos(\lambda \cdot x) - \sin(\lambda \cdot x)]$ with $\lambda = \sqrt[4]{\frac{k_w}{4 \cdot E_r I_r}}$

Position of the first root (zero-point): $w(x) = \frac{2 \cdot \lambda}{k_w} (R_r + \lambda \cdot M_r) \cdot e^{-\lambda x} \cdot \cos(\lambda \cdot x) - \frac{2 \cdot \lambda^2 \cdot M_r}{k_w} \cdot e^{-\lambda x} \cdot \sin(\lambda \cdot x) = 0$

$\Rightarrow (R_r + \lambda \cdot M_r) \cdot \cos(\lambda \cdot x) - \lambda \cdot M_r \cdot \sin(\lambda \cdot x) = 0 \Rightarrow \frac{R_r + \lambda \cdot M_r}{\lambda \cdot M_r} = \tan(\lambda \cdot x) \Rightarrow x_1 = \frac{\tan^{-1}\left(1 + \frac{R_r}{\lambda \cdot M_r}\right)}{\lambda}$

Integral up to the distance of the first root (= tensile stress resultant):

$$\begin{aligned}
 F_{t,90} &= \int_0^{x_1} \bar{p}(x) dx = 2 \cdot \lambda \cdot R_r \cdot \left[\frac{e^{-\lambda x}}{2 \cdot \lambda} \cdot (\sin(\lambda \cdot x) - \cos(\lambda \cdot x)) \right]_0^{x_1} + 2 \cdot \lambda^2 \cdot M_r \cdot \left[\frac{e^{-\lambda x}}{\lambda} \cdot \sin(\lambda \cdot x) \right]_0^{x_1} = \\
 &= R_r \cdot \left[\left(e^{-\lambda x_1} \cdot (\sin(\lambda \cdot x_1) - \cos(\lambda \cdot x_1)) - \frac{e^{-\lambda \cdot 0}}{1} \cdot \left(\frac{\sin(\lambda \cdot 0)}{0} - \frac{\cos(\lambda \cdot 0)}{1} \right) \right) \right] + 2 \cdot \lambda \cdot M_r \cdot \left[\left(e^{-\lambda x_1} \cdot \left(\frac{\sin(\lambda \cdot x_1)}{1} \right) - \frac{e^{-\lambda \cdot 0}}{1} \cdot \left(\frac{\sin(\lambda \cdot 0)}{0} \right) \right) \right] = 0 \\
 &= R_r + e^{-\lambda x_1} \cdot \sqrt[2]{2 \cdot \lambda^2 \cdot M_r^2 + 2 \cdot \lambda \cdot M_r \cdot R_r + R_r^2}
 \end{aligned}$$

$\Delta R_{r,s}$

Where $\Delta R_{r,s}$ represents an additional term resulting from both rib-tip force R_r and the cut-back length s